Proceedings of World Congress on Particle Technology 4 (CD-ROM),
21 - 25 July, Sydney, Australia, (2002), Paper No. 178.

DEM Analysis on Flow Patterns of Geldart's Group A Particles in Fluidized Bed

Tomonari KOBAYASHI
Sumitomo Chemical Co., Ltd., Japan
Tetuichiro MUKAI, Toshihiro KAWAGUCHI, Toshitugu TANAKA and Yutaka TSUJI
Department of Mechanical Engineering, Osaka University, Japan

ABSTRACT

A DEM model for flows of Group A particles in Geldart's classification is studied. Generally, Group A particles have small diameters, so that additional interactions between particles, such as the lubrication force due to the interstitial fluid and the adhesion (van der Waals) force due to the inter-molecular force may have a strong effect on their fluidization behavior. In this study, we study the effects of lubrication and adhesion forces between particles, with the aim of strict analysis on flow behavior of Group A particles in fluidized beds. The calculated results for Group A particles show the existence of the non-bubbling (homogeneous) regime, between the minimum fluidization velocity u_{mf} and the minimum bubbling velocity u_{mb}, which is a characteristic feature of Group A particles in gas fluidized beds. The corresponding experiment is made and the results are compared with the calculated ones. The values of u_{mf} and u_{mb} predicted by the DEM model with the adhesion force quantitatively agree with the experimental result.

INTRODUCTION

Gas-solid fluidized beds are widely used for catalytic reaction, polymerization, combustion, drying, granulation, coating and so on. In such granular processes, it is important to know the flow behavior of particles in fluidized beds. It is known that the fluidization behavior in gas-solid fluidized beds depends on the particle diameter and density. Geldart[1] classified powders into four groups, i.e., C, A, B and D, based on their fluidization behavior (**Fig. 1**). Group A particles have relatively small diameters and are readily fluidized.

The discrete element method (DEM) was proposed by Cundall and Strack[2]. In this method, the motion of individual particle is obtained by solving Newton's equations of motion. Over the past decade, numerical simulations of fluidized beds using DEM have been performed.[3] Although many studies have been made on the DEM simulation of fluidized beds, most of them are restricted to the bed of relatively large particles (Group B or D particles), and there are few studies for small particles such as Group A particles. However, Group A

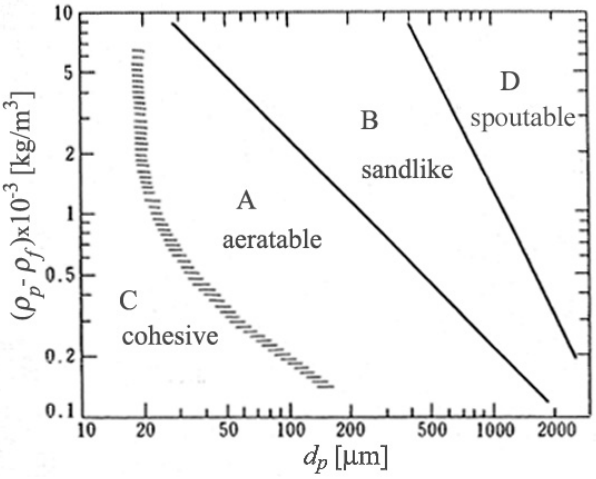

Fig. 1 Geldart's classification

particles are widely used in various industrial applications, especially catalytic reaction processes. Rhodes et al.[4] have shown that the transition of fluidization behavior from Group B to A takes place when the cohesive interparticle force is approximately equal to the single particle gravity. Xu, et al.[5] have shown that with increasing the magnitude of van der Waals forces the fluidization behavior changes from group B to A and then C.

In the present study, we investigate a discrete particle model for flows of Group A particles. Generally, Group A particles have small diameters, so that not only the adhesion force but also the lubrication force due to the interstitial fluid may play a significant role.

In this study, we study the effects of lubrication and adhesion forces between particles on the fluidized behavior predicted by a DEM-coupled-with-CFD simulation, and make quantitative validation. First, we compared the calculated pressure drop profiles with the experimental ones in a small calculation domain.

In the future, we will calculate larger calculation domain, and will compare the calculated flow patterns with the experimental ones.

CALCULATION

MOTION OF FLUID

The locally averaged equations are solved to calculate the fluid motion, taking into account the interaction between fluid and particles.[6]

Equation of continuity:

$$\frac{\partial}{\partial t}\varepsilon + \frac{\partial}{\partial x_i}(\varepsilon u_i) = 0 \tag{1}$$

Equation of motion:

$$\frac{\partial}{\partial t}(\varepsilon u_i) + \frac{\partial}{\partial x_j}(\varepsilon u_i u_j) = -\frac{\varepsilon}{\rho_f}\frac{\partial p}{\partial x_i} + \frac{\beta}{\rho_f}(\overline{v_{pi}} - u_i) \tag{2}$$

where p, u_i, v_{pi}, ε and ρ_f are the pressure, fluid velocity, particle velocity, void fraction and fluid density, respectively. The coefficient β is given by Ergun equation[7] for the dense region and Wen and Yu's equation[8] for the dilute region.

$$\beta = \begin{cases} \dfrac{\mu(1-\varepsilon)}{d_p^2\varepsilon}[150(1-\varepsilon) + 1.75\,\mathrm{Re}] & (\varepsilon \le 0.8) \\ \dfrac{3}{4}C_D\dfrac{\mu(1-\varepsilon)}{d_p^2}\varepsilon^{-2.7}\,\mathrm{Re} & (\varepsilon > 0.8) \end{cases} \tag{3}$$

$$C_D = \frac{24(1 + 0.15\,\mathrm{Re}^{0.687})}{\mathrm{Re}} \tag{4}$$

$$\mathrm{Re} = \frac{\left|\overline{\boldsymbol{v}_p} - \boldsymbol{u}\right|\rho_f \varepsilon d_p}{\mu} \tag{5}$$

where C_D is the drag coefficient for a single sphere, d_p is the particle diameter, and μ is the viscosity.

The semi-implicit method for pressure-linked equations (SIMPLE) scheme[9] is used to solve the above equations.

MOTION OF PARTICLE

The motion of the particles is calculated by solving Newton's equation of motion. In addition to the contact force $\boldsymbol{f}_C$, the fluid drag force $\boldsymbol{f}_D$, and the gravity force $\boldsymbol{f}_G$, we consider the lubrication force $\boldsymbol{f}_L$ and the adhesion force $\boldsymbol{f}_A$ in this study. The motion of particles is calculated by solving the following equation.

$$\ddot{\boldsymbol{x}} = (\boldsymbol{f}_C + \boldsymbol{f}_D + \boldsymbol{f}_G + \boldsymbol{f}_L + \boldsymbol{f}_A) / m \tag{6}$$

where m is the mass of a particle.

Contact force and fluid drag force

The contact forces are given by the conventional DEM model. The parameters in the model are given according to the method by Tsuji et al.[3]

The fluid force acting on a particle is the sum of the fluid drag force and the pressure force, and given as follows.

$$\boldsymbol{f}_D = \left[\frac{\beta}{1-\varepsilon} (\boldsymbol{u} - \boldsymbol{v}_p) - \frac{\partial p}{\partial \boldsymbol{x}} \right] V_p \tag{7}$$

where V_p is the volume of the particle, $\boldsymbol{v}_p$ is the velocity of the particle, and β is the fluid drag coefficient at the cell for fluid calculation contains the particle.

Lubrication force

The lubrication force $\boldsymbol{f}_L$ between a couple of particles is given by lubrication theory[10].

$$\boldsymbol{f}_L = -\frac{3\pi\mu a^2 \boldsymbol{v}_{app}}{2 l_{app}} \tag{8}$$

where a is the radius of the particles, l_{app} is the gap between the particles, $\boldsymbol{v}_{app}$ is their relative velocity in the normal direction.

The lubrication force between a particle and a wall is given by the following equation.

$$\boldsymbol{f}_L = -\frac{6\pi\mu a^2 \boldsymbol{v}_{napp}}{l_{napp}} \tag{9}$$

where l_{napp} is the gap between the particle and the wall, $\boldsymbol{v}_{napp}$ is their relative velocity in the normal direction.

Adhesion force

According to Seville et al.[11], spherical particles of diameter of order 100 μm should exhibit van der Waals forces to equal their single particle weight. The mean diameter of the particle in this study is 66μm, so that adhesion force $\boldsymbol{f}_A$ is given by the following equation.

$$|\boldsymbol{f}_A| = mg \tag{10}$$

Calculation conditions

The calculation conditions are shown in Table 1 and 2. As summarized in Table 2, three cases of calculations are performed in this study.

Table 1. Calculation conditions (1)

	Group-A	Grop-B
Particle diameter [μm]	66	500
Particle density [kg/m^3]	2470	
Number of particles	870	
Coefficient of friction[-]	0.3	
Coefficient of restriction [-]	0.9	
Spring constant [N/m]	1000	
Calculation time step [s]	3.8×10^{-7}	5.0×10^{-6}
Calculation domain [mm]	1.98×19.8	15×80
Superficial gas velocity [m/s]	0.004~0.012	0.13~0.45

Table 2. Calculation conditions (2)

	(α)	(β)	(γ)
Adhesion	×	O	×
Lubrication	×	×	O

○ : Considered
× : Not considered

EXPERIMENTAL

The experimental apparatus is shown in **Fig. 2**. The fluidization column is composed of a glass tube of 30mm-ID. Air is supplied to the bed through a packed bed. The air flow rate is measured by a rotameter. Glass particles are used and its mean diameter is 66μm. The pressure gradient in the bed is measured using a couple of static pressure probes.

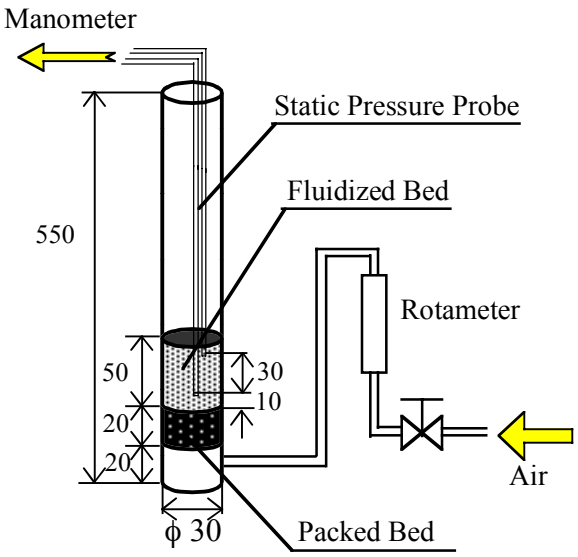

Fig. 2 Experimental apparatus

RESULTS AND DISCUSSIONS

COMPARISON OF GROUP A AND B PARTICLES

The characteristic fluidization behavior of Group A particles is the existence of the non-bubbling regime in the region between the minimum fluidization velocity u_{mf} and the minimum bubbling velocity u_{mb}. (i.e., for Group A particles, $u_{mb}/u_{mf}>1$; for Group B particles, $u_{mb}/u_{mf}=1$.) In order to determine the u_{mf} and u_{mb}, the relationship of the bed pressure drop versus the gas superficial velocity is generally used. For ideal fluidization, when the superficial gas velocity u_0 is increased from zero, the bed pressure drop Δp increases, and bed expansion occurs at u_{mf} and the pressure drop levels off beyond u_{mf}, because it reaches the

total weight of the particles in the bed. When the gas flow is decreased from the bubbling regime, the pressure drop begins to decrease at u_{mb}. (12)

First, we compare the calculation results of Group A particles with Group B particles predicted by using the DEM model (α) in which additional interparticle forces are not considered. **Fig. 3** shows the pressure drop as a function of superficial gas velocity normalized by u_{mf} (u_{mf} =6.0×10^{-3}m/s for Group A particles; u_{mf} =0.28m/s for Group B particles). This figure shows that the DEM model without any additional forces can express the Group A particles' feature in u_0-Δp diagram, i.e., in the case of Group A particles, a distinct difference between the increasing-u_0 profile and the decreasing-u_0 one can be observed.

To investigate the motion of the particles quantitatively, the RMSs of the fluctuation of void fraction and the particle velocity in the bed are analyzed. **Fig. 4** shows the RMS of the fluctuation of void fraction in the bed ($\sqrt{\overline{\varepsilon'^2}}$) as a function of superficial gas velocity. In the fixed bed or non-bubbling regime, $\sqrt{\overline{\varepsilon'^2}}$ is small because of the homogeneous distribution of ε, whereas in the bubbling regime it increases due to generated bubbles. For Group B particles $\sqrt{\overline{\varepsilon'^2}}$ begins to increase significantly around u_{mf}. This means that the non-bubbling regime does not exist. On the other hand, for Group A particles it begins to increase significantly around 1.7 u_{mf}. This result implies that the transition from uniform to bubbling regime occurs around 1.7 u_{mf}.

Fig. 5 shows the RMS of particle velocity normalized by u_{mf} as a function of superficial gas velocity. It should be noted that the RMS of particle velocity is normalized by u_{mf} (u_{mf} =6.0×10^{-3}m/s for Group A particles; u_{mf} =0.28m/s for Group B particles). For Group B particles the RMS of particle velocity begins to increase around u_{mf}. On the other hand, for Group A particles it begins to increase significantly around 1.4u_{mf}.

The results of Group A particles in **Figs. 4** and **5** show that there are two kinds of transition in the state of the particles' motion. First, around u_0/u_{mf}=1.4, the motion of the particles becomes active without making large structures such as

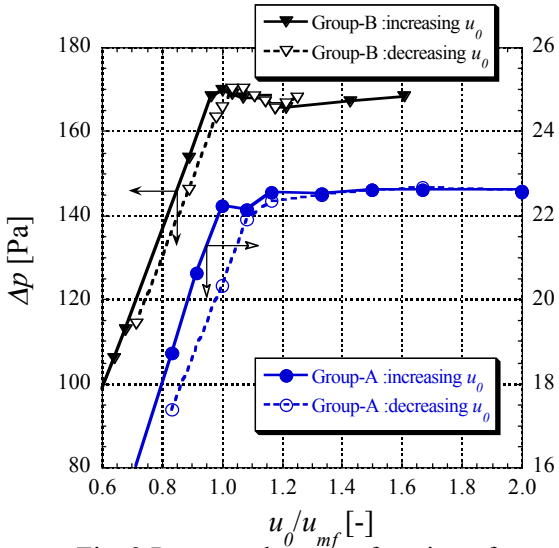

Fig. 3 Pressure drop as a function of superficial gas velocity.

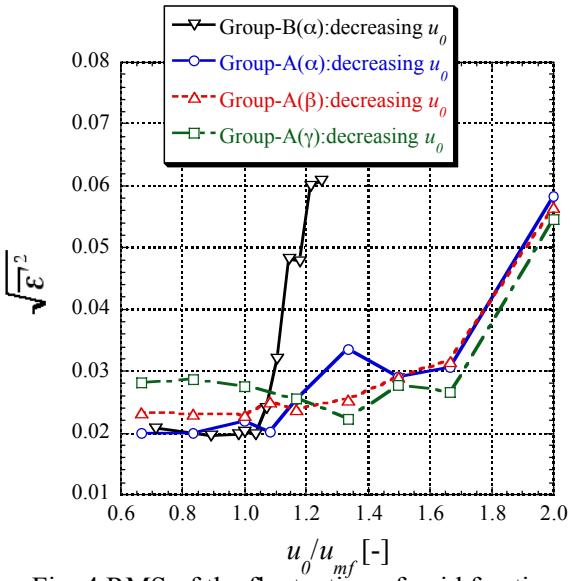

Fig. 4 RMS of the fluctuation of void fraction as a function of superficial gas velocity.

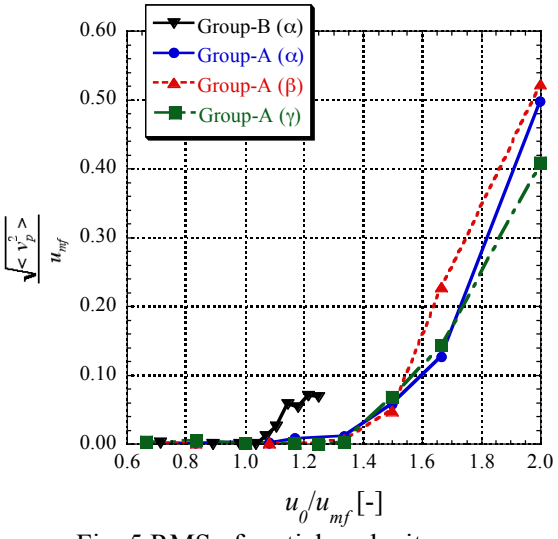

Fig. 5 RMS of particle velocity as a function of superficial gas velocity.

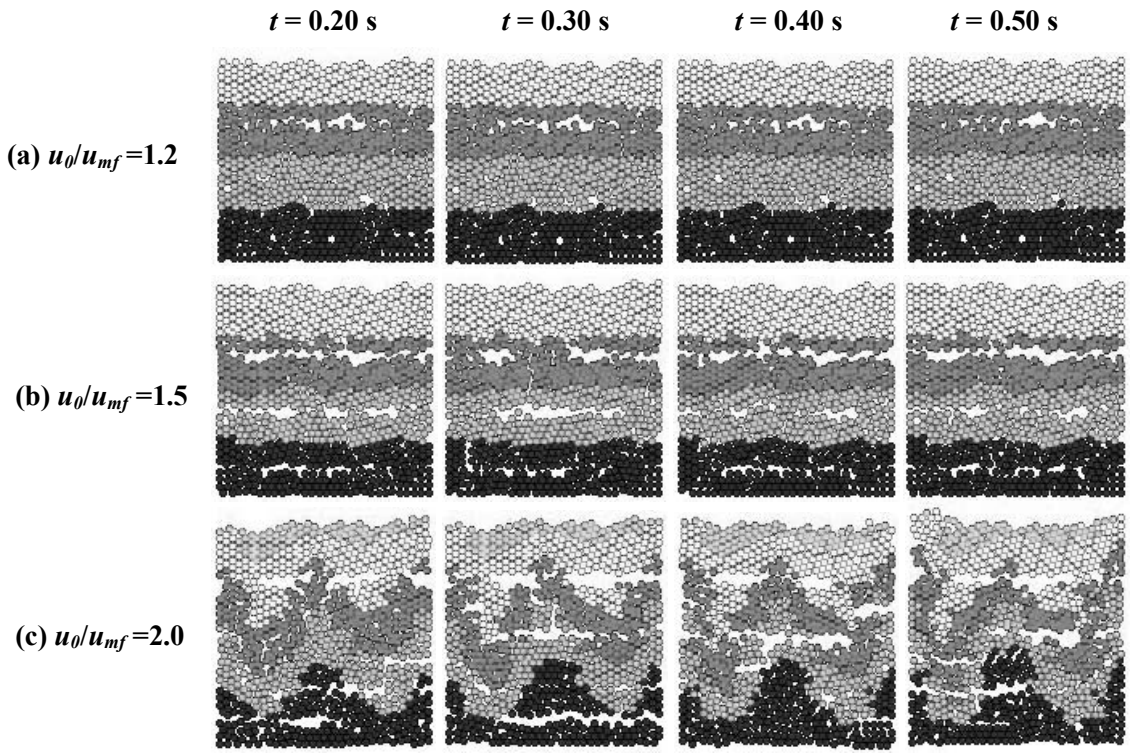

Fig. 6 Snapshots of Group A particles' motion calculated by the DEM model (α) without any additional forces.

bubbles. Secondly, around u_0/u_{mf} =1.7, the particles begin to make large structures. The transition can be explained by the observation of particles' motion.

Fig. 6 shows snapshots of Group A particles' motion calculated by the DEM model (α) without any additional forces. When u_0/u_{mf} =1.5, small-scale particle motion is observed in **Fig. 6**(b). In this case, the particle motion is restricted to its neighborhood, and large-scale deformation of particle bed is not observed. When u_0/u_{mf} =2.0, the motion of particles becomes more active, and convection of particles is observed in **Fig. 6**(c). This change of particles' motion corresponds to the results of **Figs. 4** and **5**.

The calculated results of RMSs of the fluctuation of void fraction and the particle velocity considering adhesion and lubrication forces are shown in **Figs. 4** and **5**. From those figures, additional interparticle forces have little effect on those quantities.

EFFECT OF ADHESION FORCE AND LUBRICATION FORCE

Fig. 7 shows the calculated pressure drop Δp in the bed as a function of the superficial gas velocity u_0. From this result it is found that both of the adhesion and lubrication forces have no effect on the increasing-u_0 profile and the value of u_{mf}. On the other hand, both of them have an effect on the decreasing-u_0 profile when the gas flow is

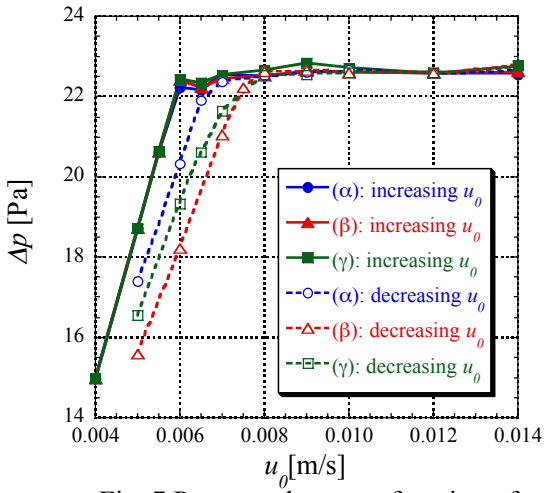

Fig. 7 Pressure drop as a function of superficial gas velocity.

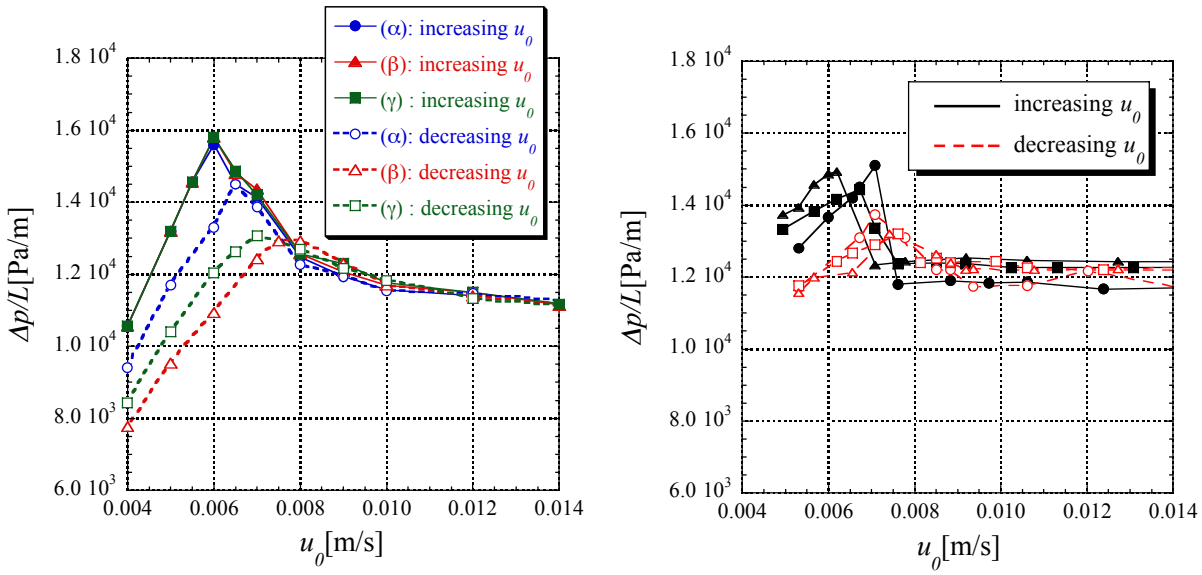

(a) Simulation (b) Experiment

Fig. 8 Pressure gradient as a function of superficial gas velocity

progressively decreased from the bubbling regime.

Fig. 8 shows the pressure gradient in the bed as a function of the superficial gas velocity. **Fig. 8** (a) shows the calculated result and **Fig. 8** (b) shows the experimental result, respectively.

Even though very small calculation region is used in the simulation, the experimental result could be expressed by the simulation quantitatively, and the calculation results clearly show the difference between the increasing-u_0 profile and decreasing-u_0 one as found in the experiment. The value u_{mf} of the experimental results agrees with the calculated ones. The DEM model with the adhesion force (β) gives the best agreement with the experimental one.

CONCLUSIONS

DEM models for flows of Group A particles in Geldart's classification have been investigated. It is found that by using the DEM model without any additional forces (α) we can express well the decreasing-u_0 profile of the Group A particles in the relationship between superficial gas velocity u_0 and pressure drop Δp. To investigate the motion of particles quantitatively, the RMSs of the fluctuation of void fraction and particle velocity have been analyzed. The calculated results of Group A particles show that there could be two kinds of transition in the state of the fluidized particles' motion. First, the motion of the particles becomes active without making large structures such as bubbles. Secondly, the particles begin to make large structures. The transition can be explained by the observation of Group A particles' motion calculated by the DEM model without any additional forces.

Effects of lubrication and adhesion forces on fluidized behavior of Group A particles have been investigated with respect to the relationship between u_0 and Δp. This result shows that both of the adhesion and lubrication forces do not affect the increasing-u_0 profile, but the decreasing-u_0 profile. The DEM model with the adhesion force (β) gives the best agreement with the experimental one.

REFERENCES

1. Geldart, D. (1973), *Powder Technology*, **7**, p285.
2. Cundall, P.A. and Strack, O.D.L. (1979), *Geotechnique*, **29**, 47p.
3. Tsuji, Y., Kawaguchi, T. and Tanaka, T. (1993), *Powder Technology*, **77**, 79p.
4. Rhodes, M.J., Wang, X.S., Nguyen, M., Stewart, P. and Liffman, K. (2001), *Chemical Engineering Science*, **56**, 69p
5. Xu, B.H., Yu, A.B. and Zulli, P. (2001), *Proc. of the fourth international conference on micromechanics of granular media (Powder and Grains 2001)*, Sendai, 577p.
6. Anderson, T.B. and Jackson, R. (1967), *I&EC Fundamentals*, **6**, 527p.
7. Ergun, S. (1952), *Chem. Eng. Prog.*, **48**, 89p.
8. Wen, C. Y. and Yu, Y. H. (1966), *Chem.Engng.Prog.Symp.Ser.No.62*, **62**, 100p.
9. Patanker, S.V. (1980), *Numerical Heat Transfer and Fluid Flow.* (Hemisphere, New York, U.S.A.)
10. Nihon-Jyunkatsugakkai (1987) *Jyunkatsu Handbook*, (Yokendo, Tokyo, Japan) (in Japanese)
11. Seville, J.P.K., Willett, C.D. and Knight, P.C. (2000), *Powder Technology.*, **113**, 261p.
12. Tsinontides, S.C. and Jackson, R. (1993), *J. Fluid Mech.*, **255**, 237p.